Article

Journal of Vibration and Control
2024, Vol. 30(7-8) 1604–1620

DOI: 10.1177/10775463231166187
journals.sagepub.com/home/jvc
Sage

Fractional-Order sliding mode control of a 4D memristive chaotic system

Abdullah Gokyildirim[1], Haris Calgan[2], and Metin Demirtas[2]

Abstract

Chaotic systems depict complex dynamics, thanks to their nonlinear behaviors. With recent studies on fractional-order nonlinear systems, it is deduced that fractional-order analysis of a chaotic system enriches its dynamic behavior. Therefore, the investigation of the chaotic behavior of a 4D memristive Chen system is aimed in this study by taking the order of the system as fractional. The nonlinear behavior of the system is observed numerically by comparing the fractional-order bifurcation diagrams and Lyapunov Exponents Spectra with 2D phase portraits. Based on these analyses, two different fractional orders (i.e., $q = 0.948$ and $q = 0.97$) are determined where the 4D memristive system shows chaotic behavior. Furthermore, a single state fractional-order sliding mode controller (FOSMC) is designed to maintain the states of the fractional-order memristive chaotic system on the equilibrium points. Then, control method results are obtained by both numerical simulations and different illustrative experiments of microcontroller-based realization. As expected, voltage outputs of the microcontroller-based realization are in good agreement with the time series of numerical simulations.

Keywords

chaos theory, fractional-order, sliding mode control, Lyapunov exponents, bifurcation

1. Introduction

In the last decade, enrichments of the dynamical behavior of nonlinear systems by performing fractional-order analysis have become a phenomenon (Xiang-Rong et al., 2008; Yang and Wang, 2021). The chaos that can be observed in many nonlinear systems depicts more complex behavior with fractional-order analysis (Ahmad and Sprott, 2003; Liu et al., 2021). Recently, many researchers have been interested in the study of fractional-order chaotic systems (Akgül et al., 2022; Chen et al., 2013; Li et al., 2020; Peng et al., 2020; Trikha et al., 2022; Zhang and Zhou, 2007). The main reason for this attraction lies in the fact that some differential systems' behavior varies chaotically in the case of particular fractional orders. Even if parameters of the nonlinear system are chosen appropriate as original form, the fractional order parameter affects the behavior of the system directly. Therefore, the well-known chaotic systems were studied in terms of complexity by means of fractional degree analysis, such as Lorenz system (Mathiyalagan et al., 2015), Lü system (Lu, 2006), Chua's system (Hartley et al., 1995), and Chen system (Lu and Chen, 2006).

Among the classical chaotic systems, Chua's system involved the memristor as the fourth passive circuit element in 1971 (Chua, 1971). Thanks to its low power consumption and nonlinearity, memristors have become the focus of attention of researchers (Itoh and Chua, 2008; Strukov et al., 2008). Therefore, there are many memristor-based chaotic systems in the literature, such as the simplest chaotic circuit (Muthuswamy and Chua, 2010), a simple memristive circuit (Bao et al., 2011), a physical circuit that employs the four passive circuit elements (Muthuswamy, 2010), and a hyperchaotic jerk system (Wang et al., 2017). Furthermore, the fact that chaotic systems are based on flux-controlled memristor makes this type of circuit easier to implement (Bao et al., 2018; Gokyildirim, Yesil and Babacan, 2022a). Recently, researchers have investigated fractional-order memristive systems with a single unstable equilibrium point (Rahman et al., 2021), bursting and boosting phenomena (Borah and Roy, 2021), and multiple coexisting analyses (Hu et al., 2021). However, most of the studied fractional-order chaotic systems do not provide dynamic analyses which include bifurcation diagrams and Lyapunov exponents. Furthermore, implementation of fractional-order

[1]Department of Electrical and Electronics Engineering, Bandirma Onyedi Eylul University, Balikesir, Turkey
[2]Department of Electrical and Electronics Engineering, Balikesir University, Balikesir, Turkey

Received: 8 July 2022; revised: 11 February 2023; accepted: 12 March 2023

Corresponding author:
Abdullah Gokyildirim, Department of Electrical and Electronics Engineering, Bandirma Onyedi Eylul University, Balikesir 10200, Turkey,
Email: agokyildirim@bandirma.edu.tr

chaotic systems is complicated via its memory index. In this regards, digital design of fractional order chaotic system arise several advantages such as cost-effective and easy applicability. Despite the limited memory of microcontrollers, a high performance of integration of fractional-order chaotic system can be realized. The superiority of the proposed application lies on employing the STM32 processor which is powerful, low-cost, low-weight, and being programmable with MATLAB program (Gokyildirim et al., 2023). When some type of microcontrollers are utilized in implementing fractional-order chaotic system (Clemente-López et al., 2022), the problem of controlling chaotic system by applying small time-dependent perturbations becomes more complicated (Emiroglu et al., 2022). Instead of these types of microcontrollers, STM32 Nucleo board is employed to keep the states of fractional-order 4D memristive system on the equilibrium points in this study.

In 1990, the OGY method was developed to realize the control of chaos (Ott et al., 1990). Later, researchers developed many methods to control chaotic behavior, such as active (Agrawal et al., 2012), passive (Kuntanapreeda and Sangpet, 2012), time-delay feedback (Ge et al., 2014), linear feedback (Sun et al., 2009), sliding-mode (Li and Liu, 2010), nonlinear control (Boubakir and Labiod, 2022; Din et al., 2021; Kizmaz et al., 2019), and linear quadratic regulator-based control (Alexander et al., 2023). Among the nonlinear control methods, sliding mode control (SMC) has superb advantages, such as being robust against disturbances, sensor noises, and ensuring well-tracking dynamics. In this context, several techniques based on SMC have been adopted for the control of a variety of chaotic systems. Roopaei et al. (2010) implemented an adaptive SMC to control a class of unknown chaotic systems. Li et al. (2011) employed a dynamic sliding surface and formed a chatter-free SMC to control a chaotic system with uncertainties. Fuzzy SMC (Ramakrishnan et al., 2022) and LMI-based SMC (Wang et al., 2009) techniques were utilized to drive the state of nonlinear chaotic systems to defined equilibrium points in the state space. Moreover, further developments in fractional calculus have led some researchers to employ FOSMC in an integer-order chaotic system (Dadras and Momeni, 2012), classical SMC in a fractional-order chaotic system (Yin et al., 2012), or FOSMC in fractional-order chaotic systems (Yang and Liu, 2013; Balasubramaniam and Muthukumar et al., 2015). Most of the given investigations in the literature prove the accuracy of the proposed FOSMC numerically, whether the chaotic system is an integer order or not. In particular, the aforementioned FOSMC studies contain a multi-state controller that requires more computational costs in microcontroller-based applications. Compared to existing studies, the proposed control method is designed as a single-state controller to avoid complexity in computation. The superiority of the proposed control structure over the reported methods in the literature is that it forces all states to the equilibrium points by controlling a single-state of the fractional order chaotic system with a good disturbance rejection capability.

To the authors' knowledge, there is a lack of studies in the literature that focus on fractional-order Chen system based on memristor. Furthermore, the complexity of the chaotic system results in difficult to design an appropriate controller. Therefore, the significant features of this paper are reported in terms of contributions as follows:

- Fractional order analyses of the 4D memristive Chen system are performed via 2D phase portraits, Lyapunov spectra, and bifurcation diagrams.
- A significant single-state SMC is designed with a fractional-order sliding surface to control a fractional-order memristive chaotic oscillator. Moreover, the stability of FOSMC is proven with Lyapunov theorem.
- The control of the fractional-order memristive chaotic oscillator is realized experimentally by means of an STM32 Nucleo which is a low-cost, low-weight microcontroller.

This paper is organized as follows: differential equations of the fractional-order memristive chaotic system are described as well as its time series and phase planes are given in the second section. Fractional-order bifurcation diagrams and Lyapunov exponents are calculated in the third section. In the fourth section, electronic circuit of fractional-order memristive chaotic oscillator is designed. FOSMC is synthesized to investigate the control of the fractional-order system in fifth section. Numerical analyses and microcontroller-based experimental realization of the fractional-order controller are explained and realized in the sixth section. Finally, the last section provides a brief discussion and the conclusion.

2. Fractional-order 4D system based on memristor

The nonlinear equations of the memristor-based 4D Chen system are described below (Gokyildirim et al., 2022b):

$$\begin{aligned} \dot{x} &= \alpha(yk(w+d)-x) \\ \dot{y} &= (\gamma-\alpha)x - xz + \gamma y \\ \dot{z} &= xy - \beta z \\ \dot{w} &= y \end{aligned} \tag{1}$$

where $k(w + d)$ is the memductance equation, which is the ratio of voltage to current, and x, y, z, and u are the state variables. Figure 1 depicts the 2D phase planes of system (1) in the case of positive constant parameters, which are $\alpha = 4$, $\beta = 0.5$, $\gamma = 3$, $k = 0.05$, and $d = 1$ for $x(0) = 0$, $y(0) = 1$, $z(0) = 0$, and $w(0) = 0$.

We can perform fractional-order analyses to enrich the dynamical complexity of the four-dimensional memristive system. For this aim, the differential equations of fractional-order form of system (1) can be written as follows:

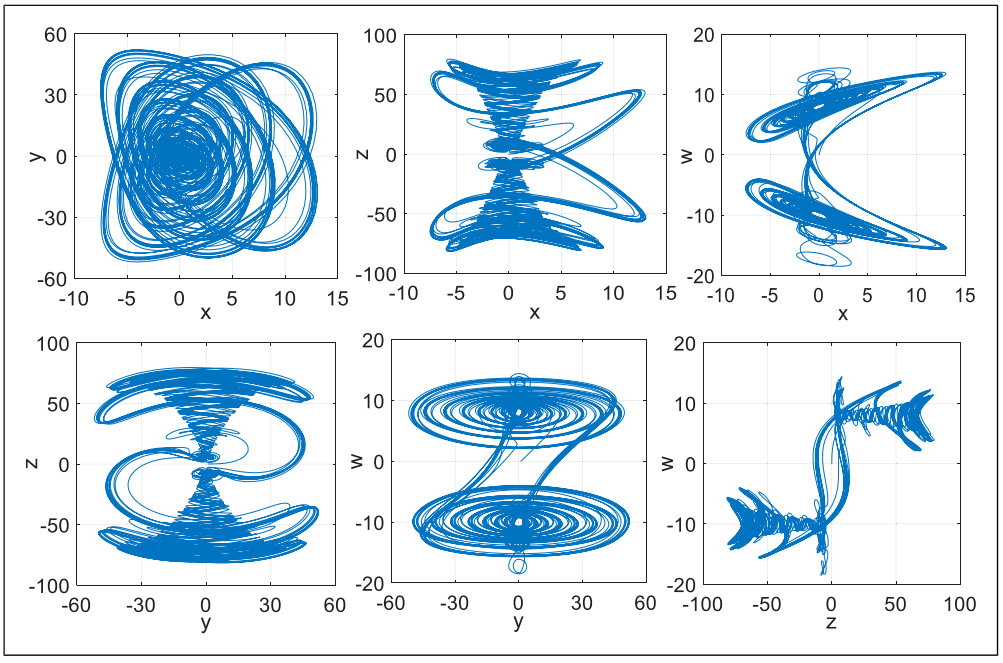

Figure 1. Phase portraits of system (1).

$$\begin{aligned} {}^{*}D^{q_1}x &= \alpha(yk(w+d)-x) \\ {}^{*}D^{q_2}y &= (\gamma-\alpha)x - xz + \gamma y \\ {}^{*}D^{q_3}z &= xy - \beta z \\ {}^{*}D^{q_4}w &= y \end{aligned} \tag{2}$$

where ${}^{*}D^{q_i}$ describes the fractional-order operator. It can be used as a non-integer differentiator or integrator by choosing the order q_i as positive or negative. Both fractional-order operators have the advantage of enhancing the characterization of the dynamic system more precisely (Han, 2021). The fractional-order operator can be determined via Grünwald–Letnikov (GL) definition as follows (Ilten, 2022):

$${}_0D_t^q f(x) = \lim_{h\to 0} \frac{1}{h^q} \sum_{k=0}^{[t/h]} (-1)^k \binom{q}{k} f(t-kh) \tag{3}$$

where [.] and h are the integer part and step size, respectively (Demirtas et al., 2019). The derivative order of 4D memristive system is dealt here as fractional-order, where $0 < q_i \leq 1$ (i = 1,2,3,4). The presence of the non-integer order integrator makes the fractional-order system (1) more flexible compared with the integer-order.

The MATLAB/Simulink program has multiple tools that are employed for fractional calculation, such as FOMCON, fid, and ninteger. The FOMCON toolbox uses the GL definition. It has a discrete integrator in particular and can be precisely implemented in digital signal processors. Therefore, it is adopted here to be used in implementing fractional-order chaotic systems. Using the FOMCON toolbox, the fractional-order 4D memristive system's time series, 2D and 3D phase portraits for $q_1 = q_2 = q_3 = q_4 = q = 0.97$ are found as illustrated in Figures 2, 3 and 4, respectively.

3. Lyapunov spectra and bifurcation diagram

In this section, the dynamic behavior of the 4D memristive system is investigated. For this aim, the Lyapunov exponents and bifurcation diagram are calculated for the varying fractional-order values of the system (2) (Messias et al., 2022). Initially, it is necessary to examine the effect of variations in the fractional-order parameter q on the system. Figures 5(a) and 5(b) depict Lyapunov spectra and bifurcation diagram for $q \in$ [0.9-1], respectively.

According to Figures 5(a) and 5(b), the fractional-order system shows some periodic oscillations for fractional-order $q \in$ ([0.913, 0.917]∪ [0.92, 0.923]∪ [0.931–-0.943]). Additionally, the fractional-order system is mostly in the chaos region when the value of q is increased from 0.944 to 0.971. Figure 5(b) demonstrates that the system depicts robust chaos for $q \in$ [0.974, 1]. According to the consistent results between the Lyapunov spectra and the bifurcation diagram, system (2) generates rich dynamic behaviors for varying values of fractional order q. Note that, the system does not represent chaotic behavior when the fractional-order is smaller than 0.905 ($q \in$ [0, 0.905]). Nevertheless, small values of fractional order require more memory index, particularly in microcontroller applications (Du et al., 2013). This memory may not be available in microcontrollers for such an

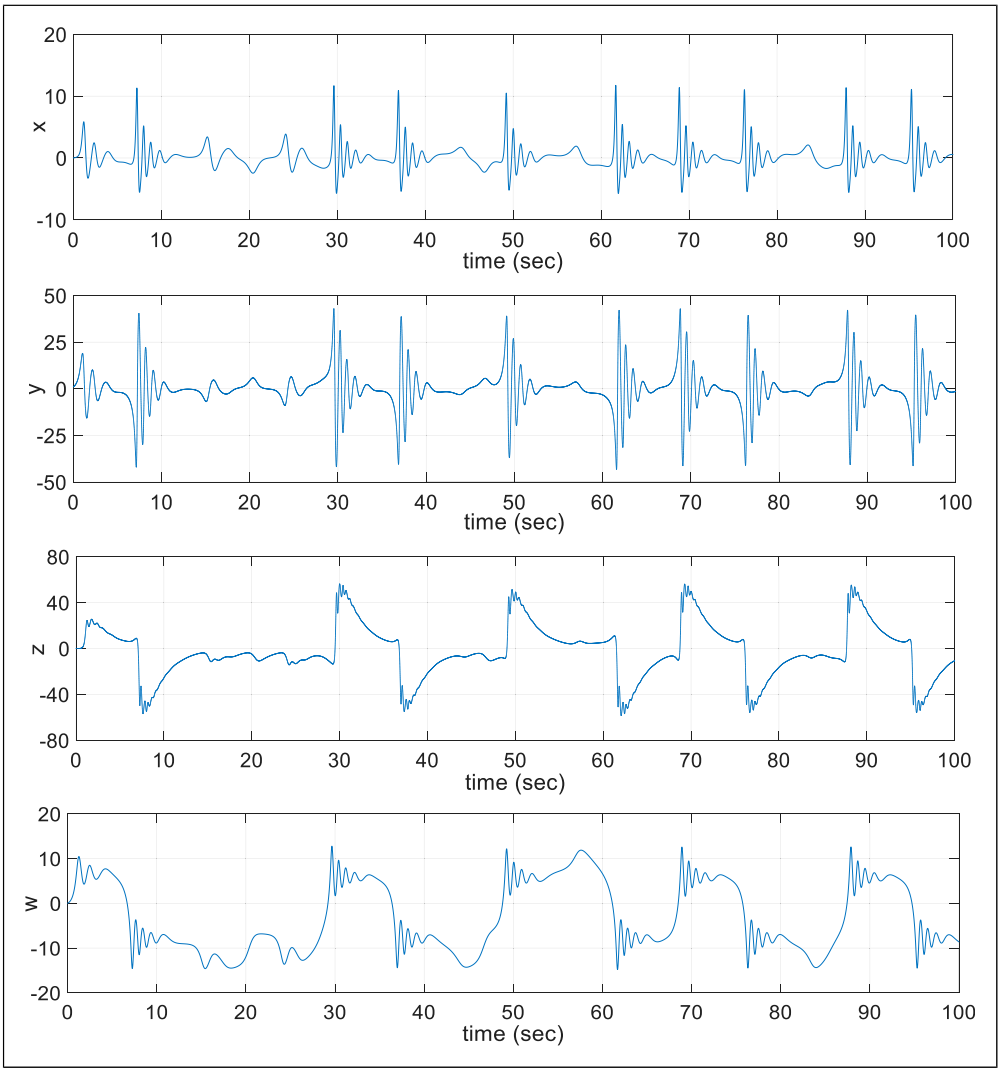

Figure 2. Time series of the memristor-based 4D fractional-order system for q = 0.97.

implementation of complex systems. Considering Figures 5(a) and 5(b), the 2D phase portraits obtained for different q values of the fractional-order system are shown in Figure 5(c). It is clearly seen from Figure 5 that the 2D phase portraits representing the system behavior are compatible with the bifurcation diagram.

The effect of varying the memristor parameter k on system (2) for a fixed fractional-order value is also investigated. According to Figure 5, the system shows chaotic motion for fractional-order q equals to 0.948 or 0.97. In Figure 6, Lyapunov exponents and bifurcation diagram are given for varying values of k when the fractional order of the system is $q = 0.948$. Here, the system is in chaos when k equals 0.05. Additionally, when the fractional-order of the system is chosen as $q = 0.97$, Lyapunov exponents and bifurcation diagram versus k are obtained as shown in Figure 7. According to Figure 7(a), the system shows chaotic behavior when $k = 0.05$. In the analyses whose results are shown in Figures 6 and 7, the parameter values are taken as $\alpha = 4$, $\beta = 0.5$, $\gamma = 3$, $d = 1$ and initial conditions are determined as $x(0) = 0$, $y(0) = 1$, $z(0) = 0$, $w(0) = 0$. According to the simulation results in this section, system (2) depicts chaotic behavior when fractional-order q is equal to 0.948 or 0.97, and a controller can be applied.

4. Electronic circuit of fractional-order memristive chaotic oscillator

An electronic circuit of fractional-order memristive 4D Chen system in OrCAD/PSpice program is designed in this section. In circuit theory, a circuit with non-integer order dynamics is called a fractance. Integer order systems can be implemented with electrical circuits using standard components that are easily available on the market. On the other hand, a fractional-order system model requires specific

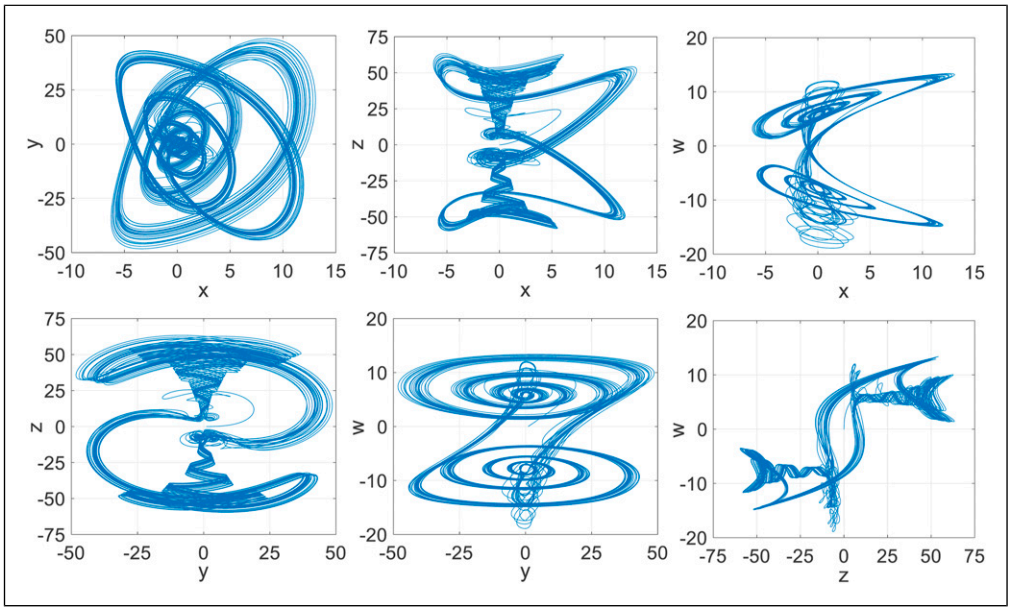

Figure 3. Phase portraits of the memristor-based 4D fractional-order system for q = 0.97.

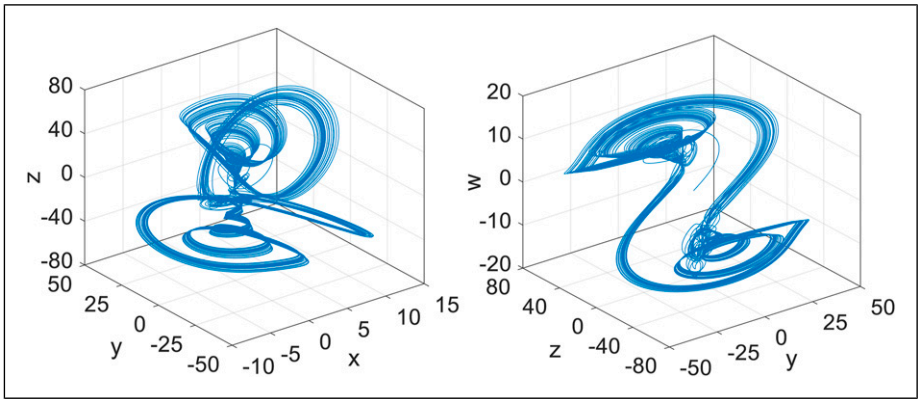

Figure 4. 3D phase portraits of the memristor-based 4D fractional-order system for q = 0.97.

resistance-capacitor (RC) circuits with fractals. The chain fractance approach, which includes two serial RC pairs, is used in this study. However, there are other approaches such as RC domino ladder and RC binary tree besides chain fractance in the literature (Yao et al., 2020). Figure 8 depicts the fractional-order integrator's circuit schematic for q = 0.97.

In order for the amplitudes of v_x, v_y, v_z, and v_w to be an acceptable range, it is necessary to scale the state variables. So, we rescale the state variables as $x = v_x/\mathrm{V}$, $y = 4v_y/\mathrm{V}$, $z = 8v_z/\mathrm{V}$, $w = 2v_w/\mathrm{V}$ (Gokyildirim et al., 2022a). Considering equation (2), Figure 9 shows the oscillator circuit schematic of the fractional-order system. Simulation time and maximum step size are 50 ms and 0.11 ms, respectively. The DC power supply voltages are also selected as $V_P = -V_N = 18V$. The circuit is simulated for the constant parameters $\alpha = 4$, $\beta = 0.5$, and $\gamma = 3$. The resistances and capacitance values of fractional-order oscillator circuit are selected as $R_1 = 100\ \mathrm{k\Omega}$, $R_2 = 20\ \mathrm{k\Omega}$, $R_3 = 1600\ \mathrm{k\Omega}$, $R_4 = 133.3\ \mathrm{k\Omega}$, $R_5 = 800\ \mathrm{k\Omega}$, $R_6 = 80\ \mathrm{k\Omega}$, $R_7 = 200\ \mathrm{k\Omega}$, $R_8 = 500\ \mathrm{k\Omega}$, $R_9 = 25\ \mathrm{k\Omega}$, $R_{10} = R_{11} = 10\ \mathrm{k\Omega}$, $R_{12} = R_{14} = R_{16} = R_{18} = 2.83\ \Omega$, $R_{13} = R_{15} = R_{17} = R_{19} = 34.838\ \mathrm{M\Omega}$, $C_1 = C_3 = C_5 = C_7 = 1.49$ nF, and $C_2 = C_4 = C_6 = C_8 = 0.905$ nF. The OrCAD/PSpice simulation results of the oscillator circuit are depicted in Figure 10. The simulation results given in Figure 10 are in good agreement with the theoretical results of the phase portraits presented in Figure 3.

5. Control of memristor-based fractional-order chaotic oscillator

This section investigates the design of FOSMC to stabilize the fractional-order 4D memristive system on a predefined

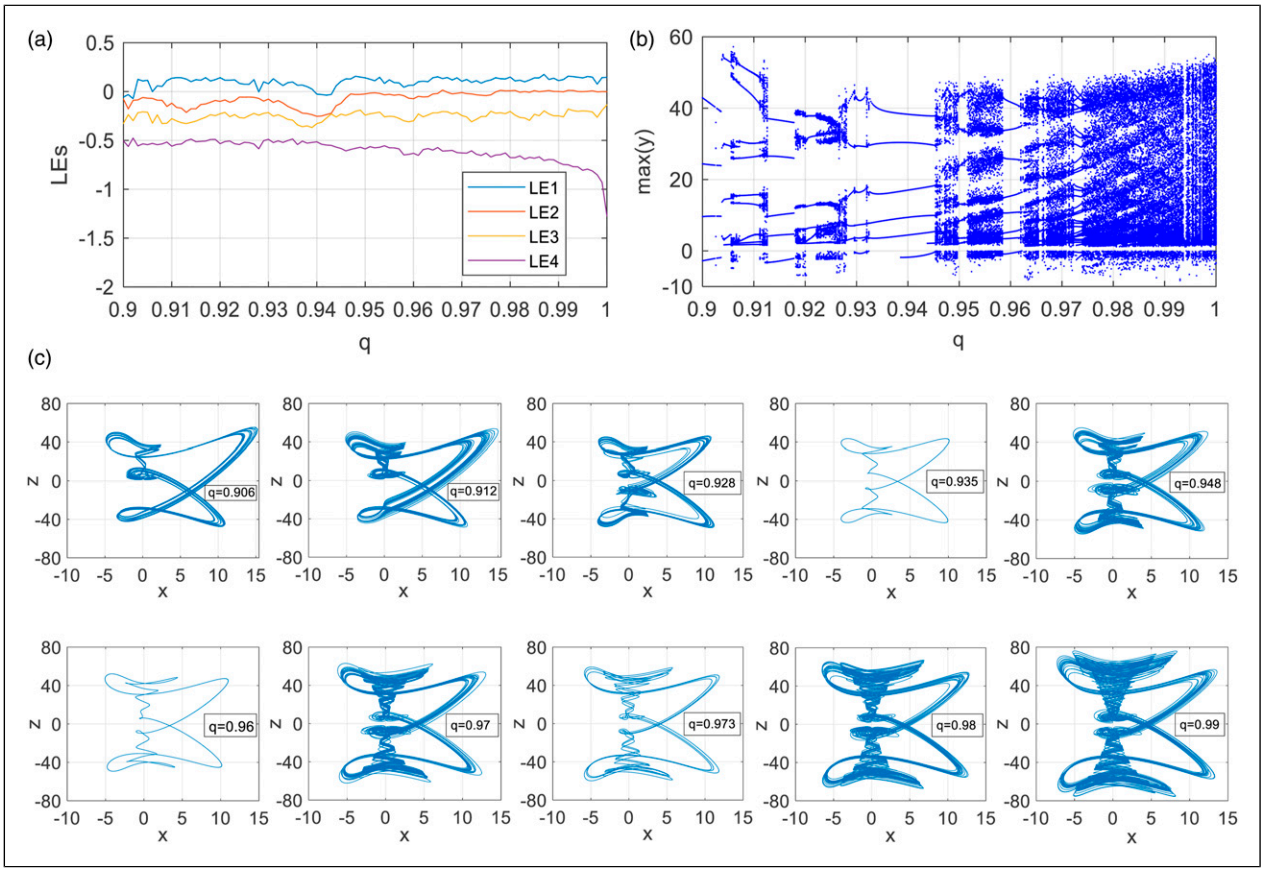

Figure 5. Spectra of Lyapunov exponents, bifurcation diagram versus varying fractional-order q and chaotic motions for parameters $\alpha = 4$, $\beta = 0.5$, $\gamma = 3$, $d = 1$ and initial conditions $x(0) = 0$, $y(0) = 1$, $z(0) = 0$, $w(0) = 0$: (a) Lyapunov exponents for $q \in [0.9, 1]$, (b) bifurcation diagram for $q \in [0.9, 1]$ versus y, (c) chaotic motions for $q \in [0.9, 1]$ when the simulation time $t(s) \in [100, 500]$.

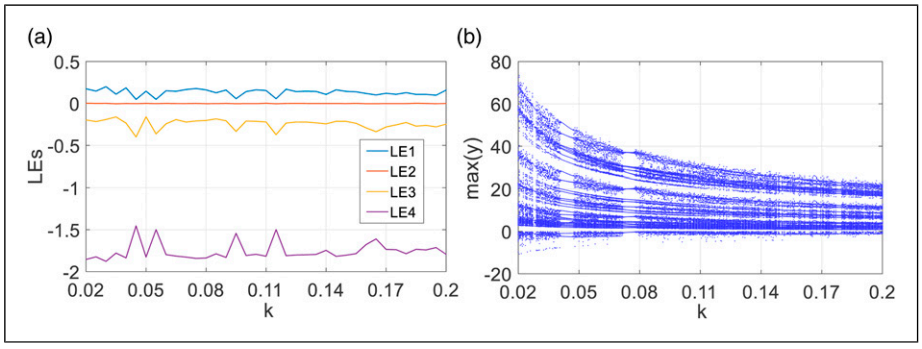

Figure 6. Spectra of Lyapunov exponents and bifurcation diagram versus varying memristor parameter k for fractional-order $q = 0.948$: (a) Lyapunov exponents for $k \in [0.02, 0.2]$ (b) bifurcation diagram for $k \in [0.02, 0.2]$ versus y.

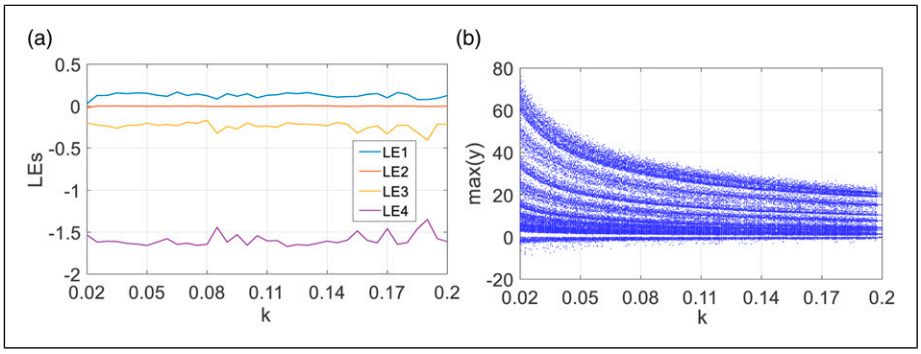

Figure 7. Spectra of Lyapunov exponents and bifurcation diagram versus varying memristor parameter k for fractional-order q = 0.97: (a) Lyapunov exponents for k ∈ [0.02, 0.2] (b) bifurcation diagram for k ∈ [0.02, 0.2] versus y.

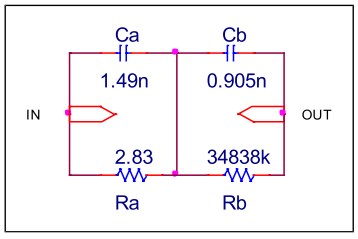

Figure 8. The fractional-order integrator's circuit schematic for q = 0.97.

equilibrium point. Since a control signal u is inserted into system (2), the state equations become as given in equation (4).

$$\begin{aligned} {}^{*}D^{q_1}x &= \alpha(k(w+d)y - x),\\ {}^{*}D^{q_2}y &= (\gamma-\alpha)x - xz + \gamma y + u,\\ {}^{*}D^{q_3}z &= xy - \beta z,\\ {}^{*}D^{q_4}w &= y. \end{aligned} \tag{4}$$

In this system, the error states vector becomes $[e_x, e_y, e_z, e_w]^T = [x, y, z, w]^T$ when the equilibrium is chosen by $E(0,0,0,0)$. By substituting equation (4) into the state vector, dynamic equations are obtained as in equation (5) since the fractional orders are taken as $q = q_1 = q_2 = q_3 = q_4 = 1$.

$$\begin{aligned} \dot{e}_x &= \alpha\big(k(e_w+d)e_y - e_x\big),\\ \dot{e}_y &= (\gamma-\alpha)e_x - e_x e_z + \gamma e_y + u,\\ \dot{e}_z &= e_x e_y - \beta e_z,\\ \dot{e}_w &= e_y. \end{aligned} \tag{5}$$

Hereby, in the following subsection, FOSMC is designed to ensure in a finite time that states of the fractional-order chaotic system attain the proposed sliding surface.

5.1. Design of fractional order sliding mode controller

The concept of the SMC has two main tasks as follows. It forces the states of the system to the previously selected surface and keeps the states in this region, respectively. To ensure that the error converges to zero, a convenient sliding surface must be determined. FOSMC has the superiorities of being more flexible via its adjustable non-integer order integrator (Calgan, 2022). Properly selected fractional-order also improves the closed-loop performance. Moreover, FOSMC shows an optimum dynamic response while containing conventional SMC benefits. Therefore, fractional-order sliding surfaces are chosen as in this study. The sliding surface is chosen as the fractional-order PI type which contains more tuning parameters to be adjusted (Zhang et al., 2012).

$$\begin{bmatrix} s_x\\ s_y\\ s_z\\ s_w \end{bmatrix} = \begin{bmatrix} K_{p1}e_x + K_{i1}D^{-\lambda}e_x\\ K_{p2}e_y + K_{i2}D^{-\lambda}e_y\\ K_{p3}e_z + K_{i3}D^{-\lambda}e_z\\ K_{p4}e_w + K_{i4}D^{-\lambda}e_w \end{bmatrix} \tag{6}$$

In equation (6), λ stands for the fractional order integral, K_p illustrates proportional gain, K_i depicts integral gain, and s demonstrates the sliding surface of each phase. Accordingly, the total sliding surface $S_T = s_x + s_y + s_z + s_w$ is selected to be zero to retain the states of the system on the surface. Afterwards, the time derivation of S_T can be taken as follows:

$$\begin{aligned} \dot{S}_T = {} & K_{p1}\dot{e}_x + K_{i1}D^{1-\lambda}e_x + K_{p2}\dot{e}_y + K_{i2}D^{1-\lambda}e_y + K_{p3}\dot{e}_z\\ & + K_{i3}D^{1-\lambda}e_z + K_{p4}\dot{e}_w + K_{i4}D^{1-\lambda}e_w \end{aligned} \tag{7}$$

Substituting the state equations in equation (5) into equation (7) results in

$$\begin{aligned} \dot{S}_T = {} & K_{p1}\big(\alpha\big(k(e_w+d)e_y - e_x\big)\big) + K_{i1}D^{1-\lambda}e_x\\ & + K_{p2}\big((\gamma-\alpha)e_x - e_x e_z + \gamma e_y + u\big)\\ & + K_{i2}D^{1-\lambda}e_y + K_{p3}\big(e_x e_y - \beta e_z\big)\\ & + K_{i3}D^{1-\lambda}e_z + K_{p4}\big(e_y\big) + K_{i4}D^{1-\lambda}e_w \end{aligned} \tag{8}$$

The equivalent control signal u_{eq} is obtained as in equation (9) when $\dot{S}_T = 0$.

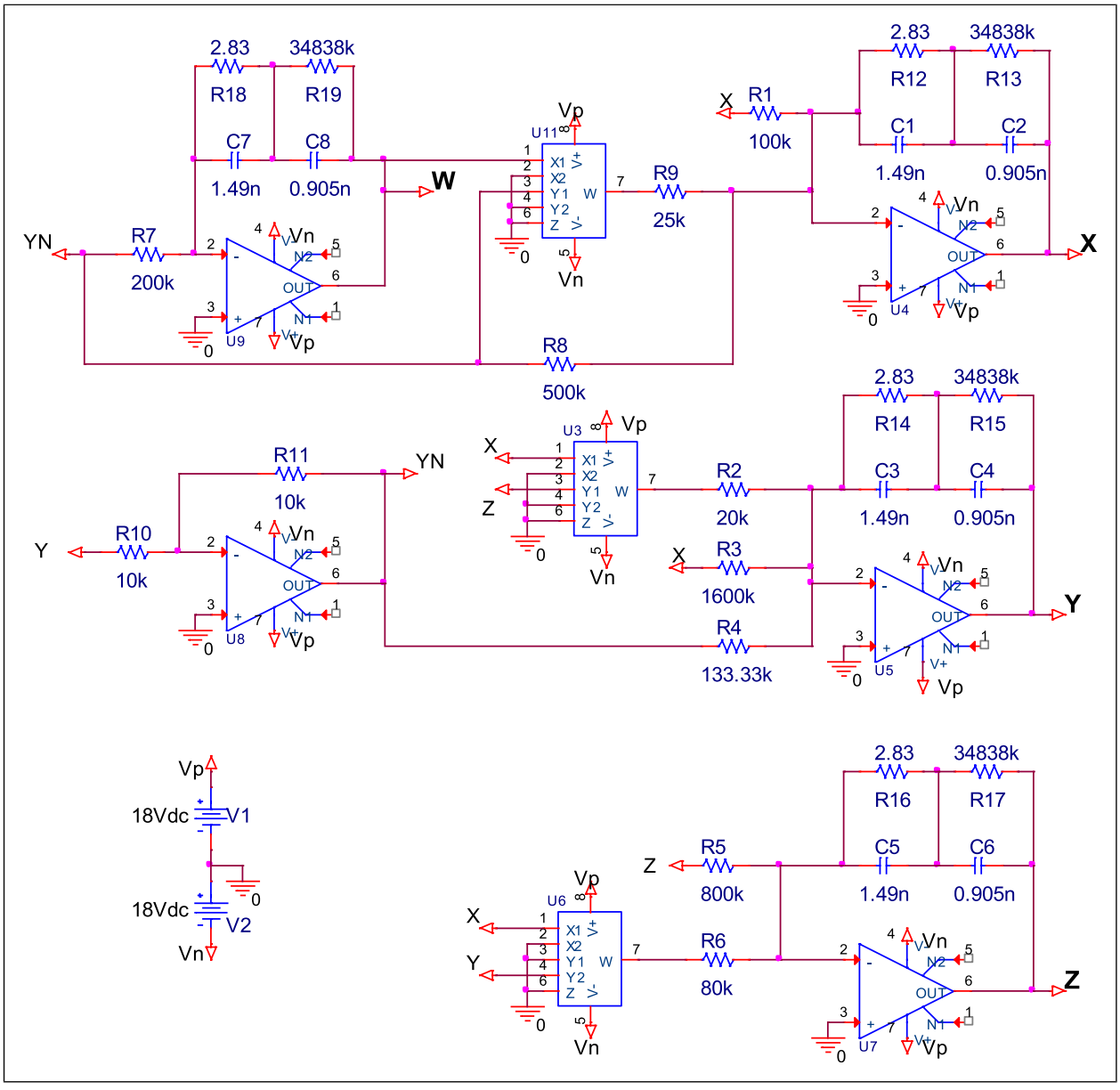

Figure 9. The fractional-order memristive oscillator's circuit schematic for q = 0.97.

$$u_{eq} = \frac{1}{K_{p2}}\left(-K_{p1}\left(\alpha k e_w + \alpha k d e_y - \alpha e_x\right) - K_{p2}\left(\gamma e_x - a e_x - e_x e_z + \gamma e_y\right) - K_{p3}\left(e_x e_y - \beta e_z\right) - K_{p4} e_y - K_{i1} D^{1-\lambda} e_x - K_{i2} D^{1-\lambda} e_y - K_{i3} D^{1-\lambda} e_z - K_{i4} D^{1-\lambda} e_w\right) \tag{9}$$

Hereby, the control signal is formed as $u = u_{eq} + u_{sw}$. u_{sw} defines the switching signal and can be written as follows:

$$u_{sw} = -\eta \mathrm{sgn}(S_T) \tag{10}$$

where η is a tunable constant. According to Lyapunov theory (V), if η is determined properly, the designed S_T converges to zero. The designed control signal u guarantees that error states in equation (5) are on the fractional-order sliding surface $S_T = 0$. To ensure the stability of the designed FOSMC, the Lyapunov function is defined as in equation (11) (Palraj et al., 2021).

$$V = \frac{1}{2} S_T^2 \tag{11}$$

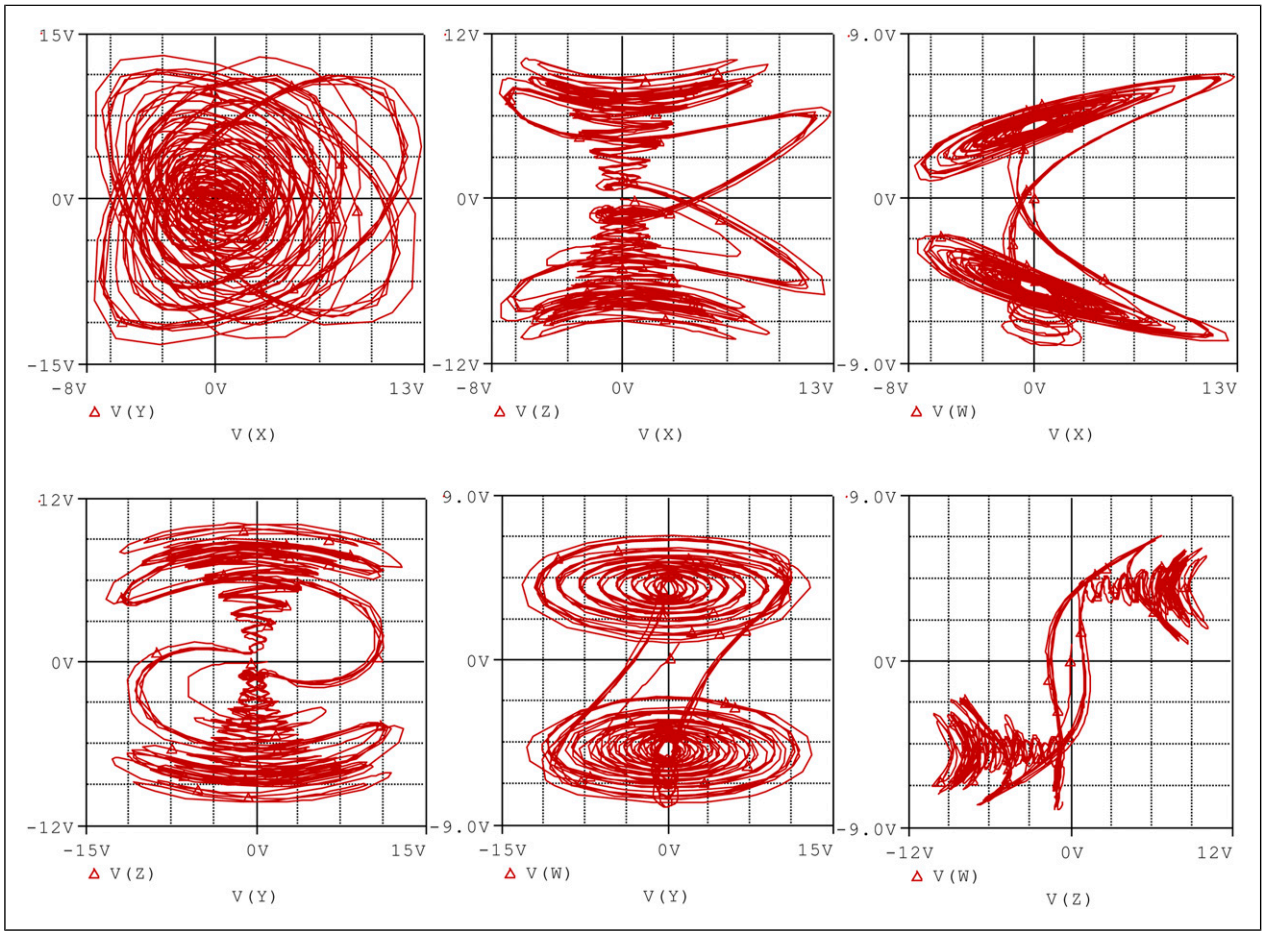

Figure 10. Phase portraits of the fractional-order memristive 4D Chen system in PSpice program for q = 0.97.

$$
\begin{aligned}
\dot{V} &= S_T(K_{p1}\left(\alpha\left(k(e_w+d)e_y-e_x\right)\right)+K_{i1}D^{1-\lambda}e_x+K_{i2}D^{1-\lambda}e_y\\
&+K_{p3}\left(e_xe_y-\beta e_z\right)+K_{i3}D^{1-\lambda}e_z+K_{p4}\left(e_y\right)+K_{i4}D^{1-\lambda}e_w\big)\\
&+K_{p2}\left((\gamma-\alpha)e_x-e_xe_z+\gamma e_y\right)\\
&+K_{p2}\left(\begin{array}{l}\dfrac{1}{K_{p2}}\begin{pmatrix}-K_{p1}\left(\alpha k e_w+\alpha k d e_y-\alpha e_x\right)-K_{p2}\left(\gamma e_x-ae_x-e_xe_z+\gamma e_y\right)\\-K_{p3}\left(e_xe_y-\beta e_z\right)-K_{p4}e_y-K_{i1}D^{1-\lambda}e_x-K_{i2}D^{1-\lambda}e_y\\-K_{i3}D^{1-\lambda}e_z-K_{i4}D^{1-\lambda}e_w\end{pmatrix}\\-\eta\mathrm{sgn}(S_T)\end{array}\right)
\end{aligned}
\tag{13}
$$

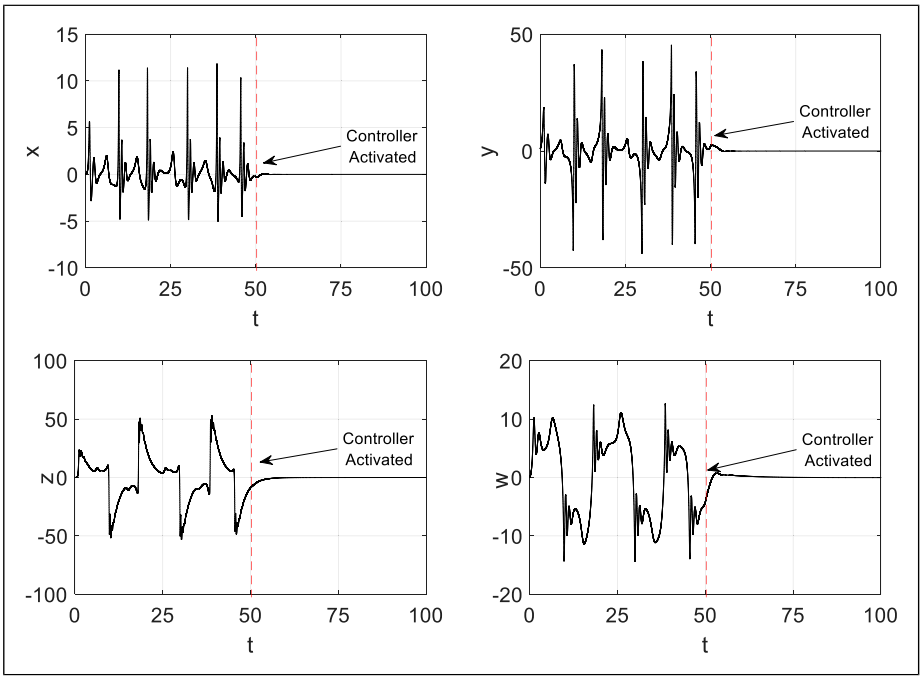

Figure 11. Simulation results for q = 0.948, k = 0.05, β = 0.5, α = 4 and, γ = 3 when the controller is activated at t = 50s.

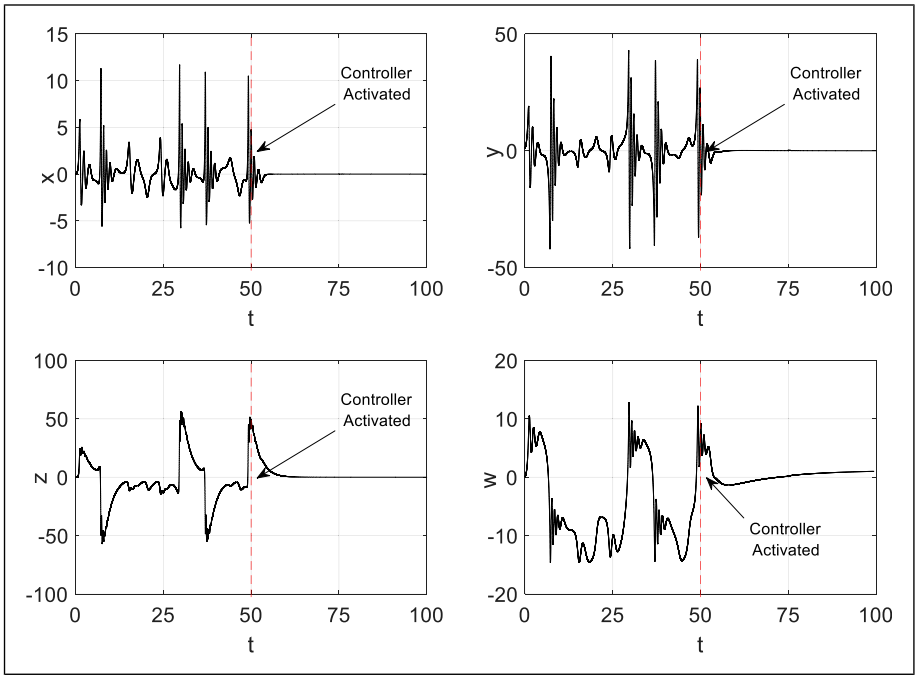

Figure 12. Simulation results for q = 0.97, k = 0.05, β = 0.5, α = 4 and, γ = 3 when the controller is activated at t = 50s.

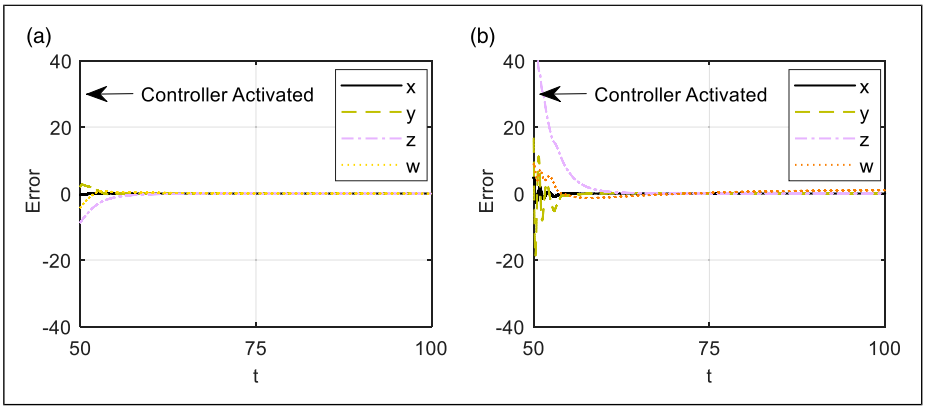

Figure 13. Error convergence curves when the controller is activated at t = 50s. (a) q = 0.948 (b) q = 0.97.

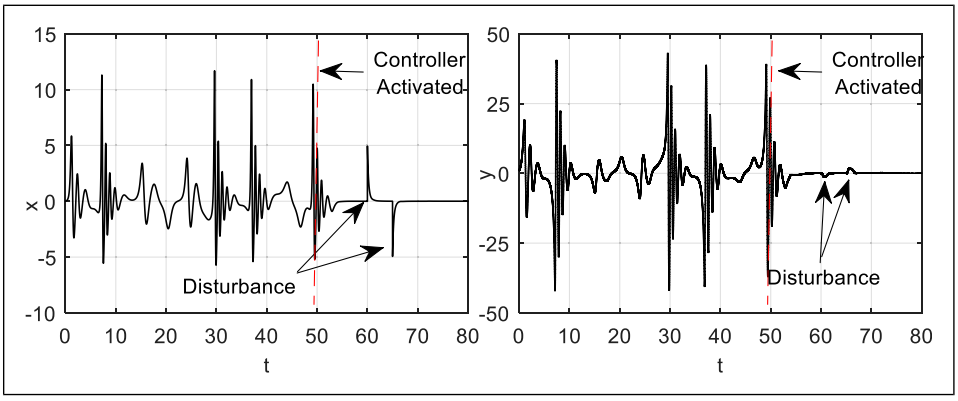

Figure 14. Robustness performance evaluation of designed controller in case of disturbance.

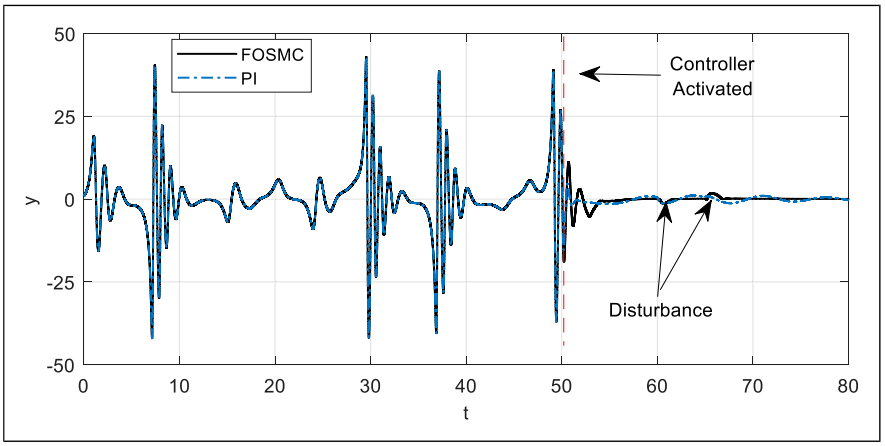

Figure 15. Comparison of FOSMC with PI controller.

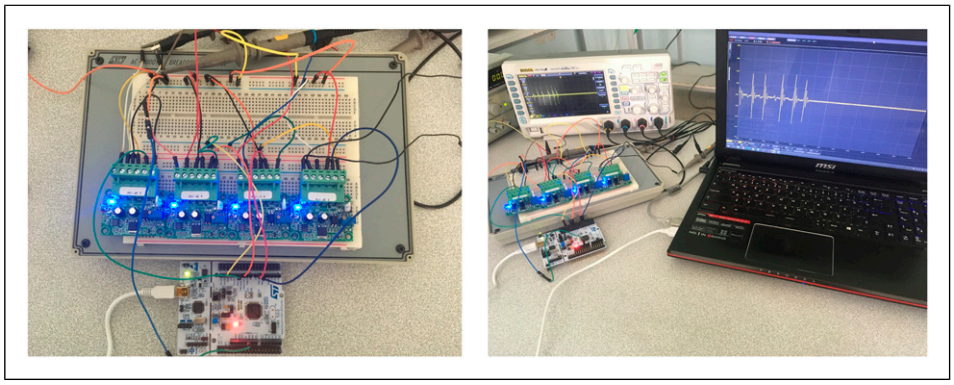

Figure 16. Microcontroller-based experimental set-up.

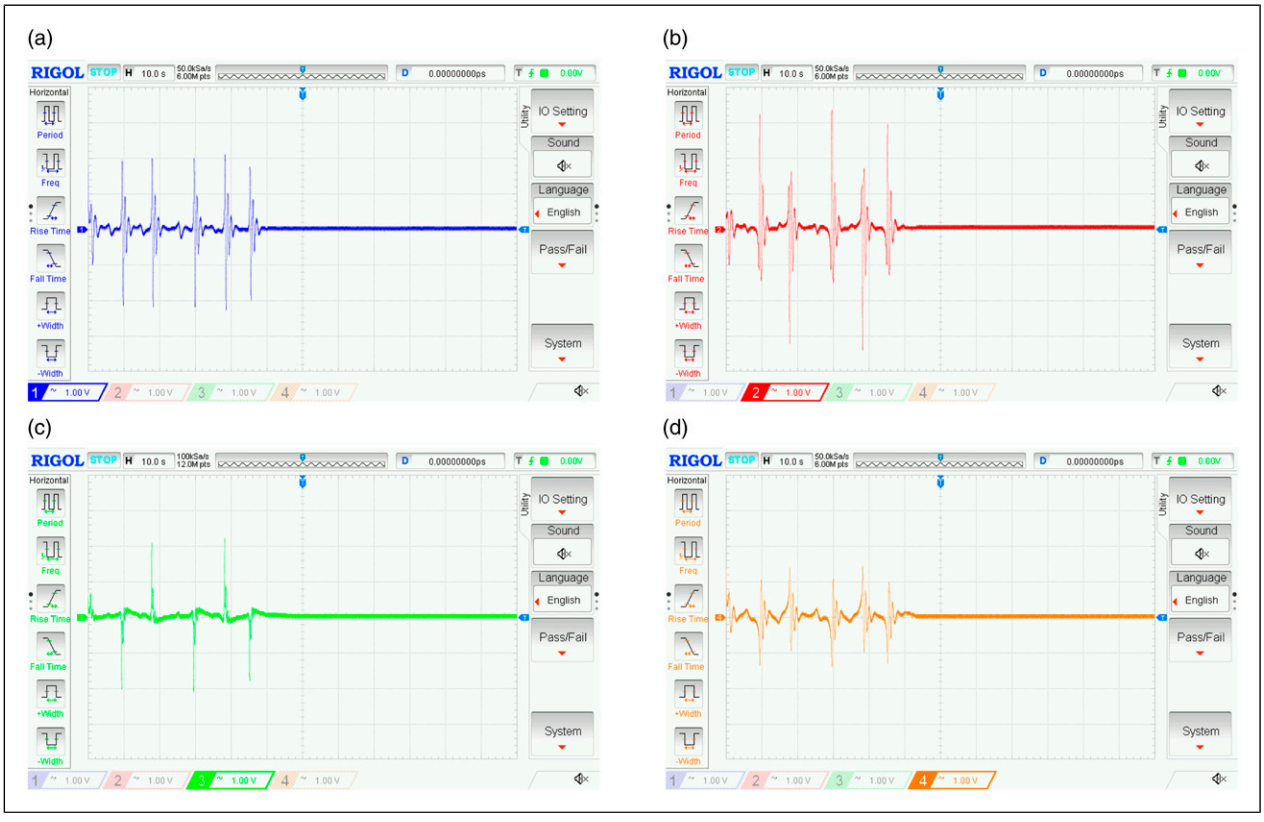

Figure 17. Experimental results for q = 0.948, k = 0.05, β = 0.5, α = 4, and γ = 3 when the controller is activated at t = 50s. Time series of the variables (a) x, (b) y, (c) z, (d) w.

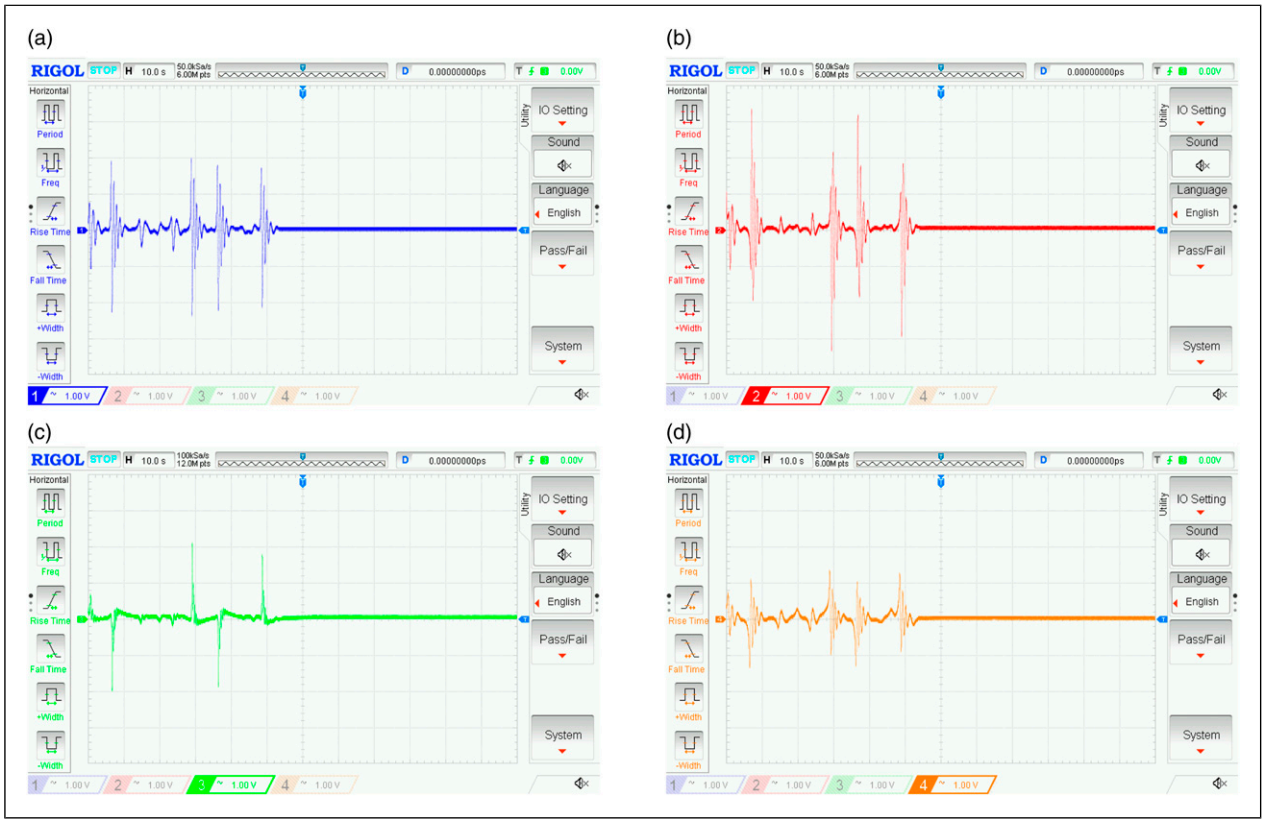

Figure 18. Experimental results for q = 0.97, k = 0.05, β = 0.5, α = 4 and γ = 3 when the controller is activated at t = 50s. Time series of the variables (a) x, (b) y, (c) z, (d) w.

Substituting equation (8) into equation (11) and taking the time derivative of the Lyapunov function yields equation (12) as follows:

$$\begin{aligned}\dot{V} &= S_T\dot{S}_T \\ &= S_T\left(K_{p1}\left(\alpha\left(k(e_w+d)e_y-e_x\right)\right)+K_{i1}D^{1-\lambda}e_x\right. \\ &\quad +K_{p2}\left((\gamma-\alpha)e_x-e_xe_z+\gamma e_y+u\right) \\ &\quad +K_{i2}D^{1-\lambda}e_y+K_{p3}\left(e_xe_y-\beta e_z\right) \\ &\quad \left.+K_{i3}D^{1-\lambda}e_z+K_{p4}\left(e_y\right)+K_{i4}D^{1-\lambda}e_w\right)\end{aligned} \tag{12}$$

Substituting u (Equations (9) and (10)) into equation (12) yields equation (13).

Consequently, the following equation is obtained when equation (13) is simplified:

$$\dot{V} = S_T\left(-K_{p2}\eta\,\mathrm{sgn}(S_T)\right) = -\rho|S_T| \le 0 \tag{14}$$

where $S_T\,\mathrm{sgn}(S_T) = |S|$ and $K_{p2}\eta = \rho$. Clearly, ρ must be strictly positive to be compatible with Lyapunov theory. Hereby, error states converge to equilibrium points by means of the designed FOSMC.

5.2. Numerical control of memristor-based fractional-order chaotic oscillator

Numerical simulations are presented in this section to verify the effectiveness of the designed FOSMC. According to the analyses in Section 3, if the non-integer orders are chosen as $q = 0.948$ and $q = 0.97$, the system in equation (2) is chaotic when the parameters α, β, γ, k, and d are 4, 0.5, 3, 0.05, and 1, respectively. The initial conditions are $x(0) = 0$, $y(1) = 0$, $z(0) = 0$, and $w(0) = 0$. Simulations are carried out on the MATLAB/Simulink program by utilizing the FOMCON fractional-order toolbox. Note that controller parameters are optimized by using integral-time absolute error (ITAE) performance criteria to fairly compare the controller performances (Calgan and Demirtas, 2021). The vector of FOSMC

gains for previously determined non-integer orders (q) is given in equation (15).

$$\begin{bmatrix} q, K_{p1}, K_{p2}, K_{p3}, K_{p4}, K_{i1}, K_{i2}, K_{i3}, K_{i4}, \lambda, \rho \\ q, K_{p1}, K_{p2}, K_{p3}, K_{p4}, K_{i1}, K_{i2}, K_{i3}, K_{i4}, \lambda, \rho \end{bmatrix}^T = \begin{bmatrix} 0.948, 9.28, 1.69, 1.02, 2.90, 0.26, 7.78, 0.10, 0.90, 0.93, 1.89 \\ 0.970, 0.78, 0.69, 0.10, 2.78, 9.39, 7.01, 0.60, 0.10, 0.71, 0.52 \end{bmatrix}^T \quad (15)$$

Simulation results for $E(0,0,0,0)$ are demonstrated in Figures 11 and 12 when the controller is implemented at $t = 50s$. It is obvious that the proposed FOSMC has great potential for controlling the fractional-order 4D memristive system. At the time $t = 50$s, each of the states heads to the equilibrium point and is kept on it for all the future time. The error figures are given in Figure 13. As proven in equation (14), all of the errors in both fractional order cases converge to zero.

The robustness performance of the designed FOSMC is tested in the case of disturbance. At $t = 60$s, a positive signal is added to the phase x as a disturbance, and a negative signal is injected after $t = 70$s. It is shown from Figure 14 that FOSMC retains the states on equilibrium points regardless of losing tracking performance. It is ensured that FOSMC acts robustly against disturbances.

PID controller is also a common control method in the literature and is widely used in control of chaotic systems (Sahin et al., 2020). Afterwards, classical PI controller is compared with designed controller taking into account tracking dynamics and disturbance rejection capability. Hence, previous simulation conditions are tackled again by means of PI controller when proportional and integral gain are chosen as 3.05, 0.9, respectively. It is shown from Figure 15 that phase y of the system heads to equilibrium point in a short time by means of PI controller. However, it contains small scale oscillations and cannot manage to keep the state on the reference quickly in case of disturbance. On the other hand, ITAE performance metric of FOSMC is calculated as 106.67 while PI controller metric is determined as 270.62. It proves that designed FOSMC has better tracking dynamics as compared to PI controller.

5.3. *Experimental realization of the fractional-order memristive chaotic oscillator by using a microcontroller*

The implementation of the memristive chaotic oscillator is performed with an STM32 F411RE Nucleo board as shown in Figure 16. Thanks to STMicroelectronics Hardware Support from Simulink, instead of complex coding, graphical programming is realized to apply the designed FOSMC. Hereby, initial values and controller parameters can be set by the user on Simulink and are deployed to the microcontroller easily. The communication between STM32 Nucleo and the computer occurs via a serial port with the RS232 protocol. The STM32 Nucleo Toolbox also provides external mode operation which offers real-time adjustment of controller parameters. When the user presses the "Start" button, the designed algorithm is compiled, downloaded to the microcontroller, and starts generating the states of the system from digital outputs. Each of the digital outputs of the STM32 Nucleo board is connected to a PWM-Analog converter through jumpers which provide analog voltage signals.

Different illustrative experiments are presented in this section to verify the effectiveness of the designed FOSMC. Considering the analyses in Section 3, the fractional-order parameter q is chosen as 0.948 or 0.97. On the other hand, the system parameters α, β, γ, k, and d are chosen as 4, 0.5, 3, 0.05, and 1, respectively, in order to achieve chaotic behavior. Controller parameters are chosen as determined in equation (15). Depending on the experimental facilities, the output of each phase must be scaled between ±3.3 V for digital application. Therefore, various scaling factors are utilized here for x, y, z, and w as 0.2, 0.06, 0.04, and 0.1, respectively. The experimental results for $E(0,0,0,0)$ are depicted in Figure 17 and Figure 18 when the controller is activated at $t = 50s$.

As expected, Figures 11–12 and Figures 17–18 show that the proposed fractional-order controller has accomplished the control of the memristive system (2). Therefore, the proposed single state control approach based on the fractional-order sliding mode method is effective for the control of the memristive chaotic attractor. Furthermore, successful operation of microcontroller-based experimental realization is occurred by means of the single state FOSMC which decreases computational complexity.

6. Conclusion

Thanks to fractional calculus, the complexity and dynamical richness of a nonlinear system increase. On the other hand, a flux-controlled memristor offers dynamical diversity due to its various properties such as nonvolatile and nonlinear behavior. Taking into account the different properties of factional-order systems and memristive structures, the fractional-order forms of a 4D chaotic system based on memristor is investigated in this study. The fractional-order system with a memristor demonstrates complex dynamic behavior, as revealed by bifurcation diagrams, Lyapunov exponent spectra, time series analyses, and phase portraits. Chaotic behavior of 4D memristive system with chosen fractional order ($q = 0.97$) is also proven with electronic circuit implementation. Additionally, the design of a FOSMC to stabilize the fractional-order 4D memristive system on a predefined equilibrium point is investigated. The superiority of the designed FOSMC is proven in terms of tracking performance and disturbance rejection while controlling a single state of the chaotic

system. Numerical simulations and different illustrative experiments of microcontroller-based realization verify the effectiveness of the designed FOSMC. Future scope of work may employ designed FOSMC in a secure communication or image encryption scheme, accurately.

Declaration of conflicting interests

The author(s) declared no potential conflicts of interest with respect to the research, authorship, and/or publication of this article.

Funding

The author(s) disclosed receipt of the following financial support for the research, authorship, and/or publication of this article: This work was supported by the Scientific Research Projects Coordination Unit of Bandırma Onyedi Eylül University (Project Number: BAP-20-1003-005).

ORCID iDs

Abdullah Gokyildirim https://orcid.org/0000-0002-2254-6325
Haris Calgan https://orcid.org/0000-0002-9106-8144

References

Agrawal SK, Srivastava M and Das S (2012) Synchronization of fractional order chaotic systems using active control method. *Chaos, Solitons & Fractals* 45(6): 737–752. DOI: 10.1016/j.chaos.2012.02.004.

Ahmad WM and Sprott JC (2003) Chaos in fractional-order autonomous nonlinear systems. *Chaos, Solitons & Fractals* 16(2): 339–351. DOI: 10.1016/S0960-0779(02)00438-1.

Akgul A, Adiyaman Y, Gokyildirim A, et al. (2022) Electronic circuit implementations of a fractional-order chaotic system and observing the escape from chaos. *Journal of Circuits, Systems and Computers* 32: 2350085.

Alexander P, Emiroglu S, Kanagaraj S, et al. (2023) Infinite coexisting attractors in an autonomous hyperchaotic megastable oscillator and linear quadratic regulator-based control and synchronization. *The European Physical Journal B* 96(1): 12.

Balasubramaniam P, Muthukumar P and Ratnavelu K (2015) Theoretical and practical applications of fuzzy fractional integral sliding mode control for fractional-order dynamical system. *Nonlinear Dynamics* 80(1–2): 249–267. DOI: 10.1007/s11071-014-1865-4.

Bao B, Ma Z, Xu J, et al. (2011) A simple memristor chaotic circuit with complex dynamics. *International Journal of Bifurcation and Chaos* 21(9): 2629–2645. DOI: 10.1142/S0218127411029999.

Bao H, Wang N, Bao B, et al. (2018) Initial condition-dependent dynamics and transient period in memristor-based hypogenetic jerk system with four line equilibria. *Communications in Nonlinear Science and Numerical Simulation* 57: 264–275. DOI: 10.1016/j.cnsns.2017.10.001.

Borah M and Roy BK (2021) Hidden multistability in four fractional-order memristive, meminductive and memcapacitive chaotic systems with bursting and boosting phenomena. *The European Physical Journal Special Topics* 230(7): 1773–1783.

Boubakir A and Labiod S (2022) Observer-based adaptive neural network control design for projective synchronization of uncertain chaotic systems. *Journal of Vibration and Control*: 107754632211019. Online ahead of print DOI: 10.1177/10775463221101935.

Calgan H (2022) Novel tilt integral sliding mode controller and observer design for sensorless speed control of a permanent magnet synchronous motor. *COMPEL - The international journal for computation and mathematics in electrical and electronic engineering* 41(1): 455–470. DOI: 10.1108/COMPEL-05-2021-0180.

Calgan H and Demirtas M (2021) Design and implementation of fault tolerant fractional order controllers for the output power of self-excited induction generator. *Electrical Engineering* 103(5): 2373–2389.

Chen D, Wu C, Iu HHC, et al. (2013) Circuit simulation for synchronization of a fractional-order and integer-order chaotic system. *Nonlinear Dynamics* 73(3): 1671–1686. DOI: 10.1007/s11071-013-0894-8.

Chua L (1971) Memristor-The missing circuit element. *IEEE Transactions on Circuit Theory* 18(5): 507–519. DOI: 10.1109/TCT.1971.1083337.

Clemente-López D, Munoz-Pacheco JM and Rangel-Magdaleno JdeJ (2022) 'A review of the digital implementation of continuous-time fractional-order chaotic systems using FPGAs and embedded hardware. *Archives of Computational Methods in Engineering* 30: 1–33.

Dadras S and Momeni HR (2012) Fractional terminal sliding mode control design for a class of dynamical systems with uncertainty. *Communications in Nonlinear Science and Numerical Simulation* 17(1): 367–377. DOI: 10.1016/j.cnsns.2011.04.032.

Demirtas M, Ilten E and Calgan H (2019) Pareto-based multi-objective optimization for fractional order $$\hbox {PI}^{\lambda }$$ PI λ speed control of induction motor by using Elman neural network. *Arabian Journal for Science and Engineering* 44(3): 2165–2175.

Din Q, Ishaque W, Iqbal MA, et al. (2021) Modification of Nicholson–Bailey model under refuge effects with stability, bifurcation, and chaos control. *Journal of Vibration and Control* 28(June): 3524–3538. DOI: 10.1177/10775463211034021.

Du M, Wang Z and Hu H (2013) Measuring memory with the order of fractional derivative. *Scientific reports* 3(1): 3431–3433.

Emiroglu S, Akgul A, Adiyaman Y, et al. (2022) A new hyperchaotic system from T chaotic system: dynamical analysis, circuit implementation, control and synchronization. *Circuit World* 48(2): 265–277.

Ge C, Hua C and Guan X (2014) Master-slave synchronization criteria of Lur'e systems with time-delay feedback control. *Applied Mathematics and Computation* 244: 895–902. DOI: 10.1016/j.amc.2014.07.045.

Gokyildirim A, Kocamaz UE, Uyaroglu Y, et al. (2023) A novel five-term 3D chaotic system with cubic nonlinearity and its microcontroller-based secure communication implementation. *AEU - International Journal of Electronics and Communications* 160: 154497.

Gokyildirim A, Yesil A and Babacan Y (2022a) Controlling a 4D chaotic oscillator with a quadratic memductance and its implementation. *Journal of Circuits, Systems and Computers* 31(16): 2250287.

Gokyildirim A, Yesil A and Babacan Y (2022b) Implementation of a memristor-based 4D chaotic oscillator and its nonlinear control. *Analog Integrated Circuits and Signal Processing* 110(1): 91–104. DOI: 10.1007/s10470-021-01956-2.

Han S-I (2021) Fractional-order sliding mode constraint control for manipulator systems using grey wolf and whale optimization algorithms. *International Journal of Control, Automation and Systems* 19(2): 676–686.

Hartley TT, Lorenzo CF and Killory Qammer H (1995) Chaos in a fractional order Chua's system. *IEEE Transactions on Circuits and Systems I: Fundamental Theory and Applications* 42(8): 485–490.

Hu Y, et al. (2021) Multiple coexisting analysis of a fractional-order coupled memristive system and its application in image encryption. *Chaos, Solitons & Fractals* 152: 111334.

Ilten E (2022) Conformable fractional order controller design and implementation for per-phase voltage regulation of three-phase SEIG under unbalanced load. *Electric Power Components and Systems* 50(11–12): 636–648.

Itoh M and Chua LO (2008) Memristor oscillators. *International Journal of Bifurcation and Chaos* 18(11): 3183–3206. DOI: 10.1142/S0218127408022354.

Kizmaz H, Kocamaz UE and Uyaroğlu Y (2019) Control of memristor-based simplest chaotic circuit with one-state controllers. *Journal of Circuits, Systems and Computers* 28(01): 1950007. DOI: 10.1142/S0218126619500075.

Kuntanapreeda S and Sangpet T (2012) Synchronization of chaotic systems with unknown parameters using adaptive passivity-based control. *Journal of the Franklin Institute* 349(8): 2547–2569. DOI: 10.1016/j.jfranklin.2012.08.002.

Li H, Liao X, Li C, et al. (2011) Chaos control and synchronization via a novel chatter free sliding mode control strategy. *Neurocomputing* 74(17): 3212–3222. DOI: 10.1016/j.neucom.2011.05.002.

Ming L and Chong-Xin L (2010) Sliding mode control of a new chaotic system. *Chinese Physics B* 19(10): 100504. DOI: 10.1088/1674-1056/19/10/100504.

Li X, Li Z and Wen Z (2020) One-to-four-wing hyperchaotic fractional-order system and its circuit realization. *Circuit World* 46(2): 107–115. DOI: 10.1108/CW-03-2019-0026.

Liu T, Yan H, Banerjee S, et al. (2021) A fractional-order chaotic system with hidden attractor and self-excited attractor and its DSP implementation. *Chaos, Solitons & Fractals* 145: 110791. DOI: 10.1016/j.chaos.2021.110791.

Lu JG (2006) Chaotic dynamics of the fractional-order Lü system and its synchronization. *Physics Letters A* 354(4): 305–311.

Lu JG and Chen G (2006) A note on the fractional-order Chen system. *Chaos, Solitons & Fractals* 27(3): 685–688.

Mathiyalagan K, Park JH and Sakthivel R (2015) Exponential synchronization for fractional-order chaotic systems with mixed uncertainties. *Complexity* 21(1): 114–125.

Messias M, Meneguette M, de Carvalho Reinol A, et al. (2022) A cubic memristive system with two twin rössler-type chaotic attractors symmetrical about an invariant plane. *International Journal of Bifurcation and Chaos* 32(13): 2230032.

Muthuswamy B (2010) Implementing memristor based chaotic circuits. *International Journal of Bifurcation and Chaos* 20(05): 1335–1350. DOI: 10.1142/S0218127410026514.

Muthuswamy B and Chua LO (2010) Simplest chaotic circuit. *International Journal of Bifurcation and Chaos* 20(5): 1567–1580. DOI: 10.1142/S0218127410027076.

Ott E, Grebogi C and Yorke JA (1990) Controlling chaos. *Physical Review Letters* 64(11): 1196–1199. DOI: 10.1103/PhysRevLett.64.1196.

Palraj J, Mathiyalagan K and Shi P (2021) New results on robust sliding mode control for linear time-delay systems. *IMA Journal of Mathematical Control and Information* 38(1): 320–336.

Peng ZW, Yu W, Wang J, et al. (2020) Dynamic analysis of seven-dimensional fractional-order chaotic system and its application in encrypted communication. *Journal of Ambient Intelligence and Humanized Computing* 11(11): 5399–5417. DOI: 10.1007/s12652-020-01896-1.

Rahman Z-ASA, Jasim BH, Al-Yasir YIA, et al. (2021) High-security image encryption based on a novel simple fractional-order memristive chaotic system with a single unstable equilibrium point. *Electronics* 10(24): 3130.

Ramakrishnan B, Cimen ME, Akgul A, et al. (2022) Chaotic Oscillations in a Fractional-Order Circuit with a Josephson Junction Resonator and its Synchronization Using Fuzzy Sliding Mode Control. *Mathematical Problems in Engineering* 2022: 11.

Roopaei M, Sahraei BR and Lin TC (2010) Adaptive sliding mode control in a novel class of chaotic systems. *Communications in Nonlinear Science and Numerical Simulation* 15(12): 4158–4170. DOI: 10.1016/j.cnsns.2010.02.017.

Sahin ME, Cam Taskiran ZG, Guler H, et al. (2020) Application and modeling of a novel 4D memristive chaotic system for communication systems. *Circuits, Systems, and Signal Processing* 39: 3320–3349.

Strukov DB, Snider GS, Stewart DR, et al. (2008) The missing memristor found. *Nature* 453(7191): 80–83. DOI: 10.1038/nature06932.

Sun M, Jia Q and Tian L (2009) A new four-dimensional energy resources system and its linear feedback control. *Chaos, Solitons & Fractals* 39(1): 101–108. DOI: 10.1016/j.chaos.2007.01.125.

Trikha P, Jahanzaib LS, Nasreen, et al. (2022) Dynamical analysis and triple compound combination anti-synchronization of novel fractional chaotic system. *Journal of Vibration and Control* 28(9–10): 1057–1073. DOI: 10.1177/1077546320987733.

Wang C, Xia H and Zhou L (2017) A memristive hyperchaotic multiscroll jerk system with controllable scroll numbers. *International Journal of Bifurcation and Chaos* 27(6): 1750091. DOI: 10.1142/S0218127417500912.

Wang H, Han Z, Xie Q, et al. (2009) Sliding mode control for chaotic systems based on LMI. *Communications in Nonlinear Science and Numerical Simulation* 14(4): 1410–1417. DOI: 10.1016/j.cnsns.2007.12.006.

Xiang-Rong C, Chong-Xin L and Fa-Qiang W (2008) Circuit realization of the fractional-order unified chaotic system. *Chinese Physics B* 17(5): 1664–1669.

Yang F and Wang X (2021) Dynamic characteristic of a new fractional-order chaotic system based on the Hopfield Neural Network and its digital circuit implementation. *Physica Scripta* 96(3): 035218. DOI: 10.1088/1402-4896/abd904.).

Yang N and Liu C (2013) A novel fractional-order hyperchaotic system stabilization via fractional sliding-mode control. *Nonlinear Dynamics* 74(3): 721–732. DOI: 10.1007/s11071-013-1000-y.

Yao J, Wang K, Huang P, et al. (2020) Analysis and implementation of fractional-order chaotic system with standard components. *Journal of Advanced Research* 25: 97–109.

Yin C, Zhong Sming and Chen W (2012) Design of sliding mode controller for a class of fractional-order chaotic systems. *Communications in Nonlinear Science and Numerical Simulation* 17(1): 356–366. DOI: 10.1016/j.cnsns.2011.04.024.

Zhang B, Pi Y and Luo Y (2012) Fractional order sliding-mode control based on parameters auto-tuning for velocity control of permanent magnet synchronous motor. *ISA transactions* 51(5): 649–656.

Zhang Y and Zhou T (2007) Three schemes to synchronize chaotic Fractional-order Rucklidge systems. *International Journal of Modern Physics B* 21(12): 2033–2044. DOI: 10.1142/S021797920703717X.